

16th CIRP Conference on Modelling of Machining Operations

An investigation of temperature and heat partition on tool-chip interface in milling of difficult-to-machine materials

Cui Di, Zhang Dinghua^{*}, Wu Baohai, Luo Ming

*Laboratory of Contemporary Design and Integrated Manufacturing Technology, Ministry of Education,
Northwestern Polytechnical University, Xi'an 710072, China*

^{*} Corresponding author. E-mail address: dhzhang@nwpu.edu.cn

Abstract

It is particularly of importance to determine temperature and heat partition on tool-chip interface in milling of difficult-to-machine materials, because they have great effect on machining process. In this paper, a new analytical method is presented to investigate temperature and heat partition on tool-chip interface in milling of difficult-to-cut materials. Besides single wire thermocouple is used to measure temperature on tool-chip interface. The tool is discretized into axial differential elements to model temperature of each differential element. The tool and chip temperature is worked out by integrating temperature of each differential element along axial direction. Secondly, Response Surface Method, an optimization method, is employed to solve heat partition on tool-chip interface. The objective function is described by matching tool and chip temperature, and the constraint condition is that heat partition cannot beyond 1. After all, the prediction temperature is compared with measurement temperature to verify this method.

© 2017 The Authors. Published by Elsevier B.V. This is an open access article under the CC BY-NC-ND license (<http://creativecommons.org/licenses/by-nc-nd/4.0/>).

Peer-review under responsibility of the scientific committee of The 16th CIRP Conference on Modelling of Machining Operations

Keywords: temperature; heat partition; difficult-to-machine materials; tool-chip interface; milling

1. Introduction

Temperature on tool-chip interface has great impact on machining operations because of its contributing to deteriorate tool wear, and reducing both the tool life and strength, especially in milling. Milling, an interrupted machining operation, is extensively used to manufacture aviation engines key parts. Tools suffer more severe thermal stress in milling than turning because they experience combination of heating-cooling and fatigue (load-unload) cycles. In milling of difficult-to-cut materials, excessively high temperature on tool-chip interface results from low thermal conductivity and intensive friction. This inevitably worsens tool wear and shortens its life to affect machining accuracy and productivity. Understandably, it is necessary to study temperature and heat partition on tool-chip interface to improve cutting condition in milling of difficult-to-machine materials.

Trigger and Chao [1] conducted pioneer research on the cutting temperature. They considered the friction heat source on tool-chip interface as moving heat source for the chip and stationary for the tool. Then using Blok's principle [2], the average temperature on contact surface for mutually contact bodies is equal, they calculated the average heat partition and temperature on tool-chip interface. Subsequently, using similar method, Loewen and Shaw [3] studied the average temperature on varying contact area. However, Trigger and Chao [4] found that the assumption about heat source uniform distribution results in inappropriate use of Blok's principle. Then they proposed a functional analysis method instead of Blok's principle to solve heat partition.

Komanduri and Hou wrote detailed review on temperature modeling. Based on heat source method, developed by Jaeger, they calculated the temperature of chip and workpiece only caused by the shear plane heat source [5]. Later, they modified Hahn and Jaeger's model to calculate the chip temperature only

considering the friction heat source in a moving coordinate system. In order to calculate the tool temperature more accurately, they considered flank face as adiabatic boundary and imaginary heat source which are not taken into account before [6]. Finally, they combined the shear plane and friction heat source to analyze the temperature on tool-chip interface and shear plane [7]. Considering the determination of heat partition, they simplified the functional analysis method developed by Trigger and Chao. After their simplification, this method becomes much faster to use [8].

Stephen and Ali [9] analyzed tool temperatures in interrupted cutting. In their work, the analytical solution in a semi-infinite rectangular corner heated by time-varying heat flux with different spacial distributions is used to investigate the tool temperature distribution.

Huang and Liang [10, 11] researched the cutting temperature under the effect of flank wear. They calculated the chip temperature considering primary shear zone as uniform moving oblique band heat source. The second deformation zone and rubbing caused by flank wear are regarded as non-uniform stationary heat source to calculate the tool temperature.

Grzesik and Nieslony [12] studied the interface temperature with multilayer coated tool at cutting speed 50-210 m/min. They analyzed heat partition to tool with various methods, including Shaw, Kato and Fuji, and Reznikov. Grzesik [13] used a hybrid analytical-FEM (finite element method) technique, i.e. boundary conditions for temperature distribution simulation are determined by analytical model, to study the temperature distribution on the cutting zone.

Abukhshim et al. [14] investigated the heat partition in high speed turning of high strength alloy steel using orthogonal cutting experiment and FEM. They found that the heat partition on tool-chip interface changes dramatically with cutting speed. Jen et al. [15] modified Stephenson's model to analyze the tool temperature under transient conditions. They used a fixed-point iteration method to work out heat partition which modified quasi-steady partition method developed by Loewen and Shaw. G.List et al. [16] researched the interface temperature and its dependency with crater wear mechanism in high speed machining. They calculated the friction shear stress and heat partition on rake face using Shaw's method, and analyzed temperature distribution under crater wear by FEM. Lazoglu and Altintas [17] developed a temperature model for tool and chip in continuous and uncontinuous machining based on finite difference method. Lin et al. [18] investigated temperature variation of workpiece in end milling, and proposed practicable algorithm of periodic temperature rise function series.

Temperature and heat partition on tool-chip interface in milling of difficult-to-machine materials have not been researched sufficiently, because of difficulties of complex tool geometry, interface area and heat flux varying dynamic. In order to overcome these difficulties, the tool is discretized into differential elements along axial direction to model its temperature. Secondly entire tool temperature is figured out by integrating all temperature of differential elements. Finally a function of heat partition is built by matching the tool and chip temperature, and solved by Response Surface Method, an optimization method.

Nomenclature

B	Heat partition to tool
α	Thermal diffusivity
λ	Heat conductivity
h_c	Deformed chip thickness
l_s	Shear plane length
l_c	Tool-chip contact length
v	Cutting speed
v_c	Velocity of chip flows
f_z	Feed per tooth
ap	Axial depth of cut
ae	Radial depth of cut
α_n	Normal rake angle
ϕ	Normal shear angle
dz	Axial integration height
K_0	Zero order modified Bessel function of the second kind
Ei	Exponential integral
Q_f	Heat generated in tool-chip interface
Q_s	Heat generated in shear plane
q_f	Heat flux on tool-chip interface
q_s	Heat flux on shear plane
T_t	Tool temperature
T_c	Chip temperature
r	Distance from any point to heat source

2. Materials and methods

2.1. Temperature modeling of tool

Some factors, including complex tool geometry and varying uncut chip thickness, make temperature modeling in milling to be more difficult. In order to overcome those, the tool is discretized into tool differential element (TDE) axially like modeling of milling forces. Fig.1 presents the analytical method carried out to determine the temperature field in the tool.

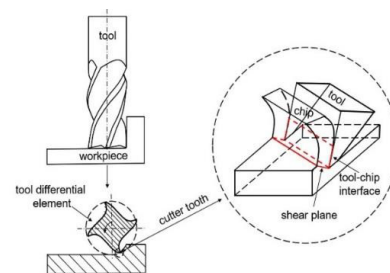


Fig. 1. Diagram of tool differential element in end milling

When the tool performs end milling, TDE independently performs oblique cutting due to helical angle. Without considering flank wear, the tool temperature is mainly affected by the friction heat source on tool-chip interface, in spite of little

part of heat generation on shear plane conducting from chip to tool [19].

Heat produced by the friction heat source is Q_f and heat partition to tool is considered as B ; the BQ_f heat is totally transmitted into the tool. Therefore, the tool-chip interface can be considered as adiabatic boundary. Due to contact with ambient air, the flank face can be considered as adiabatic boundary too. The top and bottom surface of TDE is considered as adiabatic boundary because the heat enters into each TDE in a similar way. Imaginary heat source is applied to eliminate adiabatic boundaries and the friction heat source and its imaginary heat source respect the adiabatic boundaries condition as shown in Fig.2a.

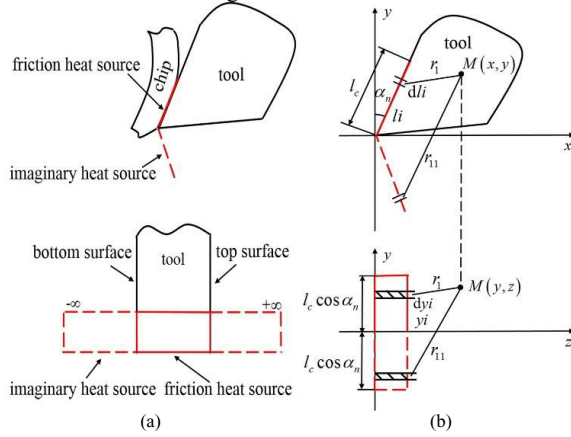


Fig. 2. Tool temperature due to friction heat source: (a) friction heat source and its imaginary heat source; (b) schematic of temperature calculation

Fig.2b presents schematic of tool temperature calculation. After imaged, the friction heat source becomes a rectangular with infinite length and width tool-chip contact length l_c . This rectangular heat source can be regarded as the sum of segments of infinite length and width dli . Therefore, the temperature solution of stationary infinite long line heat source can be considered as initial condition to calculate the tool differential element temperature. The initial condition of the calculation is

$$T = \frac{q}{2\pi\lambda} \cdot Ei \left(-\frac{r^2}{4\alpha t} \right) \quad (1)$$

Where α is the thermal diffusivity, λ is the heat conductivity, q is the heat flux of line heat source, t is the heating time, r is the distance from any point to heat source, Ei represents the exponential integral.

Thus, the temperature of tool differential element at any point $M(x, y, z)$ is

$$T_{yf} = \frac{q_f}{2\pi\lambda \cos \alpha_n} \cdot \int_{-l_c \cos \alpha_n}^{l_c \cos \alpha_n} \left[Ei \left(-\frac{r_1^2}{4\alpha t} \right) + Ei \left(-\frac{r_{11}^2}{4\alpha t} \right) \right] dy_i \quad (2)$$

Where α_n is the normal rake angle, l_c is the tool-chip contact length,

$$q_f = \frac{BQ_f}{l_c dz},$$

$$r_1 = \sqrt{(y_i - y)^2 + (x - y_i \tan \alpha_n)^2},$$

$$r_{11} = \sqrt{(y_i + y)^2 + (x - y_i \tan \alpha_n)^2}.$$

Further, the temperature of entire tool at this point can be calculated by

$$T_t = \int_0^{op} T_{yf} dz \quad (3)$$

2.2. Temperature modeling of chip

The chip temperature is mainly affected by the friction heat source on the tool-chip interface and the shear plane heat source. Firstly, the chip temperature caused by the friction heat source is analyzed. The $(1-B)Q_f$ heat is totally transmitted to the chip. The tool-chip interface can be considered as adiabatic boundary. Except for this interface, other surfaces of the chip are all in contact with the surrounding environment, therefore all of them can be considered as adiabatic boundaries. The friction heat source and its imaginary heat source are shown in Fig.3a.

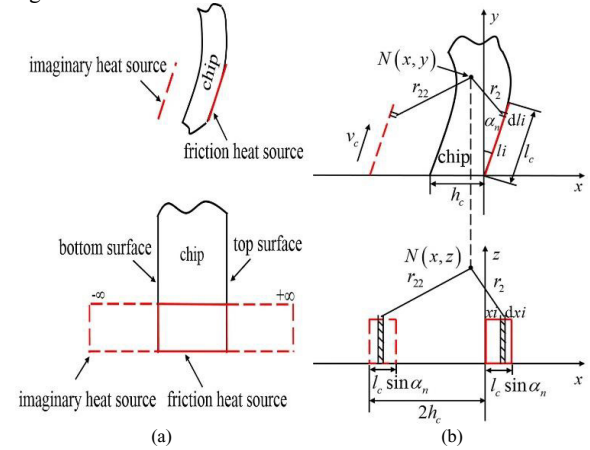


Fig. 3. Chip temperature due to friction heat source: (a) friction heat source and its imaginary heat source; (b) schematic of temperature calculation

Different from the analysis procedure of tool temperatures, the friction heat source on tool-chip interface is a moving heat source on chip; Fig.3b presents a scheme of the chip temperature calculation under those conditions. The temperature solution of a moving infinite heat source along a line can be considered as initial conditions to calculate the chip differential temperature originated from the frictional heat source. The start point of calculation is

$$T = \frac{q}{2\pi\lambda} \cdot e^{-\frac{xV}{2\alpha}} \cdot K_0 \left(\frac{rV}{2\alpha} \right) \quad (4)$$

Where X is the coordinate at the heat source moving coordinate system, V is the velocity of heat source moving, K_0 is the zero order modified Bessel function of the second kind.

Thus, the temperature of chip differential element at any point $N(x, y, z)$ is

$$T_{cf} = \frac{q_f}{2\pi\lambda \sin \alpha_n} \cdot \left[\int_0^{l_c \sin \alpha_n} e^{-\frac{(x-x_i)v_c \sin \alpha_n}{2\alpha}} \cdot K_0 \left(\frac{r_2 v_c \sin \alpha_n}{2\alpha} \right) + \int_{-2h_c}^{l_c \sin \alpha_n - 2h_c} e^{-\frac{(x-x_i)v_c \sin \alpha_n}{2\alpha}} \cdot K_0 \left(\frac{r_{22} v_c \sin \alpha_n}{2\alpha} \right) \right] dx_i \quad (5)$$

Where v_c is the velocity of chip flows, h_c is the deformed chip thickness,

$$q_f = \frac{(1-B)Q_f}{l_c dz},$$

$$r_2 = \sqrt{(y-x_i \cot \alpha_n)^2 + (x-x_i)^2},$$

$$r_{22} = \sqrt{(y-x_i \cot \alpha_n)^2 + (2h_c - x_i - x)^2}.$$

Secondly, the chip temperature caused by the shear plane heat source should be analyzed. The Q_s heat is totally conducted to chip. The shear plane heat source and its imaginary heat source respected to adiabatic boundaries are shown in Fig.4a.

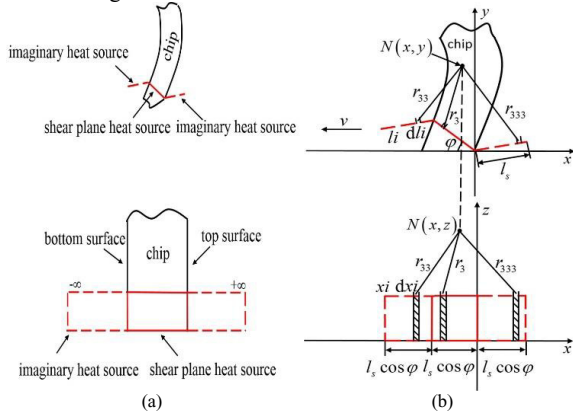


Fig. 4. Chip temperature due to shear plane heat source: (a) shear plane and its imaginary heat source; (b) schematic of temperature calculation

Fig.4b presents a scheme of the temperature calculation. The temperature of chip differential element at any point $N(x, y, z)$ is

$$T_{cs} = \frac{q_s}{2\pi\lambda \cos \phi} \cdot \left[\int_0^{l_s \cos \phi} e^{-\frac{(x-x_i)v}{2\alpha}} \cdot K_0 \left(\frac{r_3 v}{2\alpha} \right) + \int_{-l_s \cos \phi}^0 e^{-\frac{(x-x_i)v}{2\alpha}} \cdot K_0 \left(\frac{r_{33} v}{2\alpha} \right) + \int_{-l_s \cos \phi}^{-2l_s \cos \phi} e^{-\frac{(x-x_i)v}{2\alpha}} \cdot K_0 \left(\frac{r_{333} v}{2\alpha} \right) \right] dx_i \quad (6)$$

Where v is the cutting speed, l_s is the shear plane length, ϕ is the normal shear angle,

$$q_s = \frac{Q_s}{l_s dz}, \quad r_3 = \sqrt{(y-x_i \tan \phi)^2 + (y \cot \phi - x_i)^2},$$

$$r_{33} = \sqrt{(y-x_i \tan \phi)^2 + (x_i - x)^2},$$

$$r_{333} = \sqrt{(y-x_i \tan \phi)^2 + (x+x_i)^2}.$$

Further, the chip temperature caused by the friction and shear plane heat source can be calculated by

$$T_c = \int_0^{ap} (T_{cf} + T_{cs}) dz \quad (7)$$

2.3. Solution of heat partition

According to Blok's principle, the average temperature on tool and chip are equal, the heat partition to tool can be solved. However, the tool and chip temperatures in milling change with tool rotation. Therefore, this method should be modified to determine the heat partition in milling.

Using the temperature model of tool and chip has been built in section 2.1 and 2.2, the tool and chip temperatures on tool-chip interface can be determined. Based on Respond Surface Method, the function of heat partition is determined by matching tool and chip temperatures at their interface. Then a descent method is used to solve this optimization problem by minimization as

$$\min f(B) = T_t(B) - T_c(B), \quad (8)$$

s.t. $0 \leq B \leq 1$.

3. Experimental validation

Physical experiments are conducted in a four-axis machine center to measure the cutting force and temperature in milling. The experiment setup is shown in Fig.5.

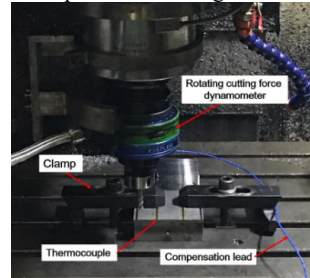


Fig. 5. Measurement of temperature and cutting force

The workpiece used in experiment is TiAl6V4, a difficult-to-cut material. A four-tooth helical end milling cutter of solid cemented carbide is selected in this paper and its diameter is 10 mm; its thermal properties are shown in Table 1.

Table 1. Thermal properties of tool and workpiece material.

Material	Heat conductivity (W/m·°C)	Thermal diffusivity (m ² /s)
TiAl6v4	8.7	3.67×10 ⁻³
Carbide	95	1.28×10 ⁻²

The cutting force is measured by a Kistler 9123C rotating cutting force dynamometer. To measure temperatures, a nickel-

chromium wire with insulation layer is used as thermocouple and embedded in workpiece with the hole of diameter 1 mm. The insulation layer is destroyed by milling action, which makes the thermocouple expose and contact with workpiece. When the tool is approaching, the temperature signal is produced [20].

In this experiment, the axial depth of cut is set as 1 mm, and the radial depth of cut is set as 2 mm. The cutting conditions are list in Table 2.

Table 2. Cutting conditions.

Run	Cutting speed (m/min)	Feed per tooth (mm)
1	60	0.15
2	80	0.15
3	100	0.15
4	60	0.20
5	80	0.20
6	100	0.20
7	60	0.25
8	80	0.25
9	100	0.25

4. Results and discussion

The necessary input parameters to calculate the temperature, including tool-chip contact length, heat and shear plane length, are worked out by analysis of the cutting force. Detailed calculation is referred to analysis of oblique cutting [21]. The cutting force coefficients are calibrated experimentally, and shown in Table 3.

Table 3. Cutting force coefficients.

Run	Cutting force coefficients		
	K_{rc}	K_{sc}	K_{ac}
1	1657	1177	195.7
2	2003	1842	382.7
3	2559	2802	327.7
4	1568	1058	206.5
5	2483	2292	232.7
6	2341	1783	622.6
7	1773	1044	115.8
8	2112	1342	181.6
9	2751	2367	301.9

Fig.6. shows that the tool-chip contact area variation at all cutting conditions. It is observed that the tendency of the contact area variation is similar in three subfigures; the increasing rate of the contact area in Fig.6a is clearly lower than Fig.6b and 6c. This is because the angle of tool rotation changes more quickly at high cutting speed than at low. Generally, in all three figures, the contact area at feed per tooth 0.25 mm is slightly bigger than at 0.2 mm or 0.15 mm. It can be explained as the larger feed per tooth causes the shear angle and uncut chip thickness increase.

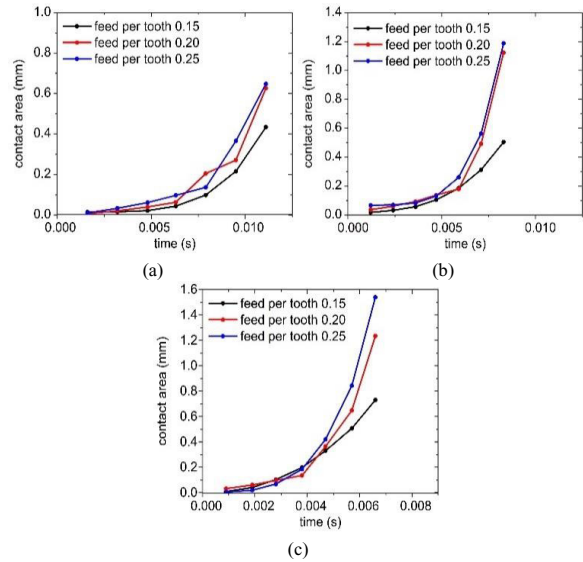


Fig. 6. Tool-chip contact area: (a) at cutting speed of 60 m/min; (b) at cutting speed of 80 m/min; (c) at cutting speed of 100 m/min

Fig.7 shows the heat partition at the tool-chip interface for all cutting conditions. Evidently, the heat partition at same cutting speed will increase together with the feed per tooth. The rise trend are totally same in the three subfigures. This because the feed per tooth has great influence on the tool-chip contact length. The cutting speed also has effect on heat partition on tool-chip interface. At same feed per tooth, the heat partition will slightly decrease with increase of the cutting speed. This because the improvement of cutting speed can make the velocity of chip flows increase which results in increase of Peclet number.

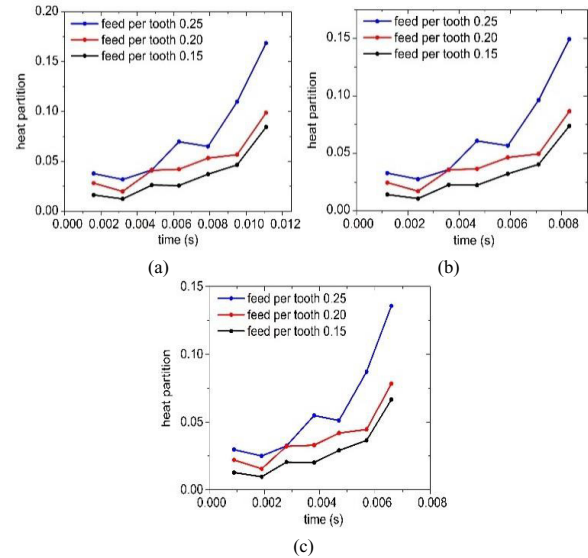


Fig. 7. Heat partition on tool-chip interface: (a) at cutting speed of 60 m/min; (b) at cutting speed of 80 m/min; (c) at cutting speed of 100 m/min

Fig.8. presents the calculated and measured temperature at all cutting conditions listed in Table 2. The theoretical results tend to be higher than the experimental results, the deviation between them is no more than 4 °C. This is because the heat generated on shear plane can conduct into tool from chip in practice, but this proportion heat fails to be taken into account in temperature model; the adiabatic boundary is assumed in temperature modeling. However, the tendency of temperature variation shows a good agreement between prediction and measurement temperature.

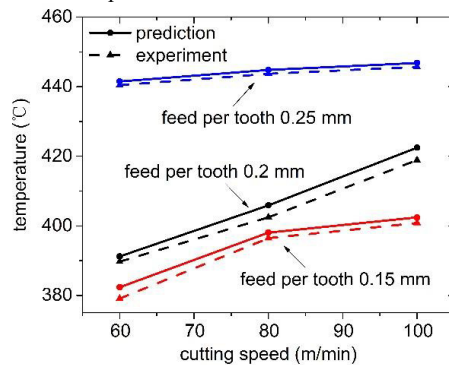


Fig. 8. Peak temperature at all cutting conditions

The figure shows that both theoretical and experimental results increase with the cutting speed increasing; when the feed per tooth improves from 0.15 to 0.25 mm, the temperature increases at same cutting speed. The feed per tooth has stronger effect on temperature than the cutting speed. At cutting speed 100 m/min, with the feed per tooth increasing from 0.15 to 0.25 mm, the temperature improves about 50 °C. However, when the cutting speed increases from 60 to 100 m/min, the temperature only improves about 20 °C at same feed per tooth. The reason partly is heat partition and heating time reduce because of the cutting speed improving; cutting forces will increase when the feed per tooth promotes.

5. Conclusion

In this study, an investigation of the temperature and heat partition on tool-chip interface is conducted in milling of difficult-to-cut materials. A new analytical model using the discrete analysis and heat source method is applied to model the chip and tool temperature and is well testified by single wire thermocouple; the heat partition is analyzed by an optimization method.

It shows a good agreement with an error no more than 4 °C to compare theoretical with experimental temperatures. The increase in tool-chip contact area presents a similar tendency at all cutting conditions, and the contact area increases more quickly at high cutting speed than at low. At same cutting speed, the heat partition will increase together with the feed per tooth. However, the heat partition at same feed per tooth will slightly decrease with the cutting speed increasing. Both the cutting speed and feed per tooth have impact on temperatures, but the feed per tooth affects more greatly on temperatures than the cutting speed.

Acknowledgements

This work is financially supported by the National Basic Research Program of China (No.2013CB035802) and National Natural Science Foundation of China (No.51475382).

References

- [1] Trigger KJ, Chao BT. An analytical evaluation of metal cutting temperature. *Trans ASME* 1950;73:57-68.
- [2] Blok HP. Theoretical study of temperature rise at surfaces of actual contact under oiliness lubrication conditions. *Proceedings of the General Discussion on Lubrication and lubricants. I Mech E, London, 1937*;2:222-235.
- [3] Loewen EG, Shaw MC. On the analysis of cutting tool temperatures. *Trans ASME* 1954;76:217-225.
- [4] Chao BT, Trigger KJ. Temperature distribution at the tool-chip interface in metal cutting. *Trans ASME* 1956;72:1107-1121.
- [5] Komanduri R, Hou ZB. Thermal model of the metal cutting process: Part 1-Temperature rise distribution due to shear plane heat source. *Int J Mech Sci* 2000;42:1715-1752.
- [6] Komanduri R, Hou ZB. Thermal model of the metal cutting process: Part 2-Temperature rise distribution due to friction heat source at the tool-chip interface. *Int J Mech Sci* 2001;43:57-88.
- [7] Komanduri R, Hou ZB. Thermal model of the metal cutting process: Part 3-Temperature rise distribution due to combined effects of shear plane heat source and the tool-chip interface frictional heat source. *Int J Mech Sci* 2001;43:89-107.
- [8] Komanduri R, Hou ZB. Analysis of heat partition and temperature distribution in sliding systems. *Wear* 2001;251:925-938.
- [9] Stephenson DA, Ali A. Tool temperatures in interrupted metal cutting. *J Eng Ind-T ASME* 1992;114:127-136.
- [10] Huang Y, Liang SY. Modeling of the cutting temperature distribution under the tool flank wear effect. *P I Mech Eng C-J Mec* 2003;217:1195-1208.
- [11] Huang Y, Liang SY. Cutting temperature modeling based on non-uniform heat intensity and partition ratio. *Mach Sci Technol* 2005;9:301-323.
- [12] Grzesik W, Nieslony P. Physics based modeling of interface temperatures in machining with multilayer coated tools at moderate cutting speeds. *Int J Mach Tool Manu* 2004;44:889-901.
- [13] Grzesik W. Determination of temperature distribution in the cutting zone using hybrid analytical-FEM technique. *Int J Mach Tool Manu* 2006;46:651-658.
- [14] Abukhshim NA, Mativenga PT, Sheikh MA. Investigation of heat partition in high speed turning of high strength alloy steel. *Int J Mach Tool Manu* 2005;45:1687-1695.
- [15] Jen TC, Anagonye AU. An improved transient model of tool temperatures in metal cutting. *J Manuf Sci E-T ASME* 2001;123:30-37.
- [16] List G, Sutter G, Bouthiche A. Cutting temperature prediction in high speed machining by numerical modeling of chip formation and its dependence with crater wear. *Int J Mach Tool Manu* 2012;54-55:1-9.
- [17] Lazoglu I, Altintas Y. Prediction of tool and chip temperature in continuous and interrupted machining. *Int J Mach Tool Manu* 2002;42:1011-1022.
- [18] Lin S, Peng FY, Wen J, Liu YZ, Yan R. An investigation of workpiece temperature variation in end milling considering flank rubbing effect. *Int J Mach Tool Manu* 2013;73:71-86.
- [19] Abukhshim NA, Mativenga PT, Sheikh MA. Heat generation and temperature prediction in metal cutting: A review and implication for high speed machining. *Int J Mach Tool Manu* 2006;46:782-800.
- [20] Wu BH, Cui D, He XD, Zhang DH, Tang K. Cutting tool temperature prediction method using analytical model for end milling. *Chinese J Aeronaut* 2016;29:1788-1794.
- [21] Altintas Y. *Manufacturing Automation: Metal cutting mechanics, Machine tool vibrations, and CNC design*. 2nd ed. Cambridge: Cambridge University Press; 2012.